Non-cyclic geometric phases and helicity transitions for neutrino oscillations in magnetic field

Sandeep Joshi* and Sudhir R. Jain†
Nuclear Physics Division, Bhabha Atomic Research Centre, Mumbai 400085, India
Homi Bhabha National Institute, Anushakti Nagar, Mumbai 400094, India
(Dated: March 16, 2017)

We show that neutrino spin and spin-flavor transitions involve non-vanishing geometric phases. Analytical expressions are derived for non-cyclic geometric phases arising due to neutrino oscillations in magnetic fields and matter. Several calculations are performed for different cases of rotating and non-rotating magnetic fields in the context of solar neutrinos and neutrinos produced inside neutron stars. It is shown that the neutrino eigenstates carry non-vanishing geometric phases even at large distances from their original point of production. Also the effects of critical magnetic fields and cross boundary effects in case of neutrinos emanating out of neutron stars are analyzed.

arXiv:1703.05027v1 [hep-ph] 15 Mar 2017

I. Introduction

The study of neutrino oscillations in vacuum, matter and magnetic fields is a widely discussed topic in high energy physics. The experimental confirmation of the neutrino oscillation hypothesis [1] proves that neutrinos are massive particles. Since the standard model (SM) assumes neutrinos to be massless, in the simplest extension of the SM, right-handed components of the neutrino fields are introduced to account for the mass of the neutrinos. In this minimally extended SM, neutrinos acquire non-zero magnetic dipole moments due to coupling with the photon at one loop level [2–4]. This results in spin and spin-flavor oscillations between left- and right-handed neutrino states in the presence of sufficiently strong magnetic fields. This possibility has been discussed both for the case of Dirac [5] and Majorana neutrinos [6]. Since the right-handed Dirac neutrino states are singlets under the $SU(2)_L$ gauge group, they do not participate in weak interactions and hence are sterile and do not show up in the experiments. For the case of Majorana neutrinos, even though diagonal magnetic moments vanish [6], there could be non-zero off-diagonal magnetic moments which result in transitions between neutrinos of different flavor and helicities, commonly termed as $\nu \leftrightarrow \bar{\nu}$ transitions. The spin and spin-flavor oscillations may also lead to resonant conversion mechanisms, similar to the Mikheyev-Smirnov-Wolfenstein (MSW) effect [7], the possibility of which has been extensively discussed in various scenarios including solar [8–18] and supernova neutrinos [19–24](see [25] for a detailed list of references).

Associated with the phenomenon of neutrino oscillations in vacuum, matter and magnetic fields is the emergence of geometric phase, which has been explored by many authors in various settings [26–41]. The concept of geometric phase emerges from the idea that the phase factor acquired by wavefunction of a system undergoing quantum evolution has a part which is dynamical and a part which is path-dependent or geometric in nature. Berry in his seminal paper [42] showed that for systems undergoing cyclic, adiabatic evolution this path-dependent geometric phase can have observable consequences. The definition of geometric phase has been subsequently generalised to include non-adiabatic, non-cyclic and non-unitary evolutions [43–46]. A particularly interesting approach of non-cyclic, non-adiabatic geometric phase based on quantum kinematics has been developed by Mukunda and Simon [47] which we follow in this paper.

The phenomena of geometric phase emerges in a wide range of classical and quantum systems and dates back to the work of Pancharatnam [48] who demonstrated that when a polarized light is passed through a series of polarizers such that initial polarization is finally restored, the final polarized state acquires an additional phase. This additional phase is equal to half the solid angle subtended by the curve representing the polarization states on a Poincaré sphere. The geometric phase since then has been observed in a wide range of systems such as molecular physics [49], neutron spin-rotation [50], photon propagation in helically wound optical fiber [51] etc. In particle physics, in addition to neutrinos, the importance of geometric phase has been explored in the context of supersymmetric quantum mechanics [52], CPT violation in meson systems [53] and axion-photon mixing [54].

In the present work we analyze the non-cyclic geometric phases that arise due to neutrino oscillations in magnetic fields and matter. In particular, we first perform explicit calculations for the geometric phases that arise due to spin and spin-flavor precession of neutrinos propagating in a medium with constant density and uniformly twisting magnetic fields. We then study the case of geometric phase acquired by neutrinos produced inside and emanating out of a neutron star, with realistic density and magnetic field profiles. We also study the condition of adiabaticity, the effects of magnetic field rotation and cross boundary effects on geometric phases and neutrino helicity transitions. This is a generalization of our previous work [39], where we calculated the cyclic Berry phase for the neutrino propagation in a magnetic field rotating

* sjoshi@barc.gov.in
† srjain@barc.gov.in

arbitrarily about the neutrino direction. In [39] it was shown that as the rotating magnetic field traces a closed curve in the parameter space, the neutrino eigenstates can develop significant geometric phase if the magnetic field is sufficiently strong ($\sim 10^7 G$ or more). Such magnetic fields are usually encountered by neutrinos propagating though astrophysical environments such as core-collapse supernova, neutron stars, gamma ray bursts etc.

The calculations pertaining to spin and spin-flavor oscillations of neutrinos depend on strength of one-loop magnetic dipole moments. In the minimally extended SM, the diagonal magnetic moments of the Dirac neutrinos to one-loop order have been calculated to be [2, 3] $\mu_\nu = 3.2\times10^{-19}(m_\nu/eV)\mu_B$, where m_ν is neutrino mass. However this value is much smaller than the sensitivity of present experiments. The current best experimental constraint on neutrino magnetic moment comes from the GEMMA experiment which puts an upper bound of $\mu_\nu < 2.9\times10^{-11}\mu_B$ [55]. A recent analysis [56] of the Borexino data obtains bound on the Majorana transition magnetic moment at $\mu_\nu \leq 3.1\times10^{-11}\mu_B$. Also there are various solar, reactor and accelerator neutrino experiments which obtain different bounds on neutrino magnetic moments [57]. On the theoretical side, various models have been proposed which derive the bounds on the neutrino magnetic moment as large as $10^{-10}\mu_B$ (see [25] for a detailed review). In this paper, we take the value of neutrino magnetic moment $\mu_\nu = 10^{-11}\mu_B$ for calculations.

II. Neutrino spin and spin-flavor evolution

In the quasiclassical approach, neutrino spin evolution in an electromagnetic field is described by generalized Bargmann-Michel-Telegdi (BMT) equation [58]. For the system $|\nu\rangle = (\nu_L, \nu_R)^T$ of two helicity components of neutrinos propagating in the presence of magnetic field $\vec{B}$ in matter, the effective Hamiltonian is given by [59]

$$H = (\vec{\sigma}.\vec{n})\frac{V}{2} - \mu\vec{\sigma}.\Big(\vec{B} - \big(1+\frac{1}{\gamma}\big)(\vec{B}.\vec{n})\vec{n}\Big), \tag{1}$$

where $\vec{n}$ is the direction of propagation of neutrino, $\vec{\sigma}$ are Pauli spin matrices and

$$V = \Delta V - \frac{\Delta m^2 A}{2E}, \tag{2}$$

with $\Delta V = V_L - V_R$; V_L, V_R being potential due to coherent forward scattering of the neutrinos with matter particles [60] for left- and right-handed neutrinos respectively , $\Delta m^2 = m_R^2 - m_L^2$, A is a function of neutrino mixing angle θ and E is the neutrino energy. In (1) the terms proportional to unity are omitted.

Assuming the neutrinos to be propagating along the z-direction, the evolution of the state $|\nu\rangle$ can be described by the schrödinger-like equation [61]

$$i\frac{\partial\,|\nu(t)\rangle}{\partial t} = H(t)\,|\nu(t)\rangle\,, \tag{3}$$

with H given by (1). Since the longitudinal component of magnetic field in (1) is suppressed by a factor $1/\gamma$, for relativistic neutrinos this term is negligible and we consider only the magnetic field rotating in transverse plane $B_\perp = Be^{i\phi}$. The evolution equation (3) can now be written as

$$i\frac{\partial}{\partial z}\begin{pmatrix}\nu_L\\ \nu_R\end{pmatrix} = \begin{pmatrix}V(z)/2 & \mu B(z)e^{i\phi(z)}\\ \mu B(z)e^{-i\phi(z)} & -V(z)/2\end{pmatrix}\begin{pmatrix}\nu_L\\ \nu_R\end{pmatrix}, \tag{4}$$

where the distance z along the neutrino trajectory is approximated with time t. Transforming to rotating frame of the field using

$$|\nu\rangle = U\,|\psi\rangle = \exp(i\sigma_3\phi/2)\,|\psi\rangle\,, \tag{5}$$

we get the evolution equation in rotating frame

$$\begin{aligned} i\frac{\partial\,|\psi\rangle}{\partial z} =& (U^{-1}HU - iU^{-1}\frac{dU}{dz})\,|\psi\rangle \\ =& \frac{1}{2}\big[(V+\dot{\phi})\sigma_3 + (2\mu B)\sigma_1\big]\,|\psi\rangle\,, \end{aligned} \tag{6}$$

where $\dot{\phi} = d\phi/dz$. For the case of neutrino propagation in matter with constant density and in magnetic field of constant strength and uniform twist i.e. constant V, B and $\dot{\phi}$, (6) can be integrated analytically and we obtain

$$\begin{pmatrix}\psi_L(z)\\ \psi_R(z)\end{pmatrix} = \exp\left[-\frac{i}{2}\Big((V+\dot{\phi})\sigma_3 + 2\mu B\sigma_1\Big)z\right]\begin{pmatrix}\psi_L(0)\\ \psi_R(0)\end{pmatrix}. \tag{7}$$

Using properties of Pauli matrices this can be written as

$$\begin{aligned} \begin{pmatrix}\psi_L(z)\\ \psi_R(z)\end{pmatrix} =& \Big[\cos\Big(\frac{\delta E_m z}{2}\Big) - \frac{i}{\delta E_m}\Big((V+\dot{\phi})\sigma_3 + 2\mu B\sigma_1\Big) \\ & \sin\Big(\frac{\delta E_m z}{2}\Big)\Big]\begin{pmatrix}\psi_L(0)\\ \psi_R(0)\end{pmatrix}, \end{aligned} \tag{8}$$

where

$$\delta E_m = \sqrt{(V+\dot{\phi})^2 + (2\mu B)^2}, \tag{9}$$

gives the energy splitting of the eigenstates. Finally, using (5) we obtain the evolution equations for the neutrino helicity states

$$\nu_L(z) = e^{i\phi/2}\Big[\big(\cos(\delta E_m z/2) - i\cos 2\theta_m \sin(\delta E_m z/2)\big)\psi_L(0) - i\sin 2\theta_m \sin(\delta E_m z/2)\psi_R(0)\Big], \tag{10}$$

$$\nu_R(z) = e^{-i\phi/2}\Big[\big(\cos(\delta E_m z/2) + i\cos 2\theta_m \sin(\delta E_m z/2)\big)\psi_R(0) - i\sin 2\theta_m \sin(\delta E_m z/2)\psi_L(0)\Big], \tag{11}$$

where θ_m is the mixing angle between ν_L and ν_R given by,

$$\tan 2\theta_m = -\frac{2\mu B}{V + \dot{\phi}}. \tag{12}$$

If a beam of left handed neutrinos start at $z = 0$, the transition probability at distance z is given by

$$P(\nu_L \to \nu_R; z) = |\nu_R(z)|^2 = \sin^2 2\theta_m \sin\left(\frac{\delta E_m z}{2}\right). \tag{13}$$

Thus neutrino propagation in magnetic fields result in oscillation in the $\nu_L - \nu_R$ basis. For $\theta_m = \pi/4$ the mixing is maximal and the amplitude of the transition probability becomes unity. (12) gives the condition for resonant $\nu_L \leftrightarrow \nu_R$ conversion

$$V + \dot{\phi} = 0, \tag{14}$$

$$\text{or} \qquad \Delta V - \frac{\Delta m^2}{2E} A + \dot{\phi} = 0. \tag{15}$$

The effects of the variation of the twisting field on the transition probability has been explored in details in [13]. If we now include the effects of the three neutrino flavor the effective Hamiltonian becomes 6×6 matrix which can be written as

$$H = H_0 + H_{wk} + H_B, \tag{16}$$

where H_0 is the vacuum term which is same for both Dirac and Majorana neutrinos, given by

$$H_0 = \frac{1}{2E}\begin{pmatrix} U & 0 \\ 0 & U \end{pmatrix}\begin{pmatrix} M^2 & 0 \\ 0 & M^2 \end{pmatrix}\begin{pmatrix} U^\dagger & 0 \\ 0 & U^\dagger \end{pmatrix}, \tag{17}$$

where M^2 is the mass matrix, $M^2 = \text{Diag}(0, \Delta m^2_{21}, \Delta m^2_{31})$ and U is the unitary mixing matrix which can be suitably parameterized. H_{wk} is the matter potential term given by

$$H_{wk} = \alpha\rho \begin{cases} \text{Diag}\big(Y_e, 0, 0, (1-Y_e)/2, (1-Y_e)/2, \\ (1-Y_e)/2\big) \quad \text{for Dirac neutrinos} \\ \text{Diag}\big(Y_e, 0, 0, 1-2Y_e, 1-Y_e, 1-Y_e\big) \\ \text{for Majorana neutrinos} \end{cases}, \tag{18}$$

where Y_e is the electron fraction, ρ is the density of the medium, and $\alpha = \sqrt{2}G_F/m_N$ is constant Finally, H_B is neutrino coupling with the magnetic field

$$H_B = \begin{pmatrix} 0 & M_\mu^\dagger B e^{i\phi} \\ \pm M_\mu B e^{-i\phi} & 0 \end{pmatrix}, \tag{19}$$

where $\pm$ sign refers to Dirac and Majorana neutrinos respectively and M_μ is the magnetic moment matrix given by

$$M_\mu = \begin{cases} \begin{pmatrix} \mu_{ee} & \mu_{e\mu} & \mu_{e\tau} \\ \mu_{e\mu} & \mu_{\mu\mu} & \mu_{\mu\tau} \\ \mu_{e\tau} & \mu_{\mu\tau} & \mu_{\tau\tau} \end{pmatrix} & \text{for Dirac neutrinos} \\ \begin{pmatrix} 0 & \mu_{e\mu} & \mu_{e\tau} \\ -\mu_{e\mu} & 0 & \mu_{\mu\tau} \\ -\mu_{e\tau} & -\mu_{\mu\tau} & 0 \end{pmatrix} & \text{for Majorana neutrinos} \end{cases} \tag{20}$$

If a neutrino is produced as left handed electron neutrino and propagates in a magnetic field, combination of diagonal and off-diagonal magnetic moments leads to the following spin and spin-flavor transitions between different neutrino states
For Dirac neutrinos: $\nu_{eL} \to \nu_{eR}, \nu_{eL} \to \nu_{\mu R}, \nu_{eL} \to \nu_{\tau R}$
For Majorana neutrinos : $\nu_{eL} \to \bar{\nu}_\mu, \nu_{eL} \to \bar{\nu}_\tau$
And the condition for resonant transitions (15) can be written as

$$\alpha\rho Y_e^{eff} - \frac{\Delta m^2 A}{2E} + \dot{\phi} = 0, \tag{21}$$

where

$$Y_e^{eff} = \begin{cases} (3Y_e - 1)/2 & \text{for} \quad \nu_{eL} \leftrightarrow \nu_{e_R, \mu_R, \tau_R} \\ (2Y_e - 1) & \text{for} \quad \nu_{e_L} \leftrightarrow \bar{\nu}_{\mu,\tau}. \end{cases} \tag{22}$$

We now examine the geometric phases associated with the spin and spin-flavor evolution of the neutrinos propagating in magnetic fields and matter.

III. Mukunda-Simon phases

Consider a quantum system whose Hamiltonian depends on a set of adiabatically varying parameters, undergoing a cyclic evolution along a closed curve in the parameter space $\mathbf{R}$. An eigenstate $|\psi(t)\rangle$ of the system acquire a geometric phase given by [42]

$$\gamma[C_R] = i\oint_{C_R} d\mathbf{R} \cdot \langle\psi(\mathbf{R})\,|\,\nabla_R\,|\,\psi(\mathbf{R})\rangle\,, \tag{23}$$

where C_R is the closed curve in the parameter space. Aharonov and Anandan [43] generalised this definition to incorporate non-adiabatic evolution. The evolution of the state $|\psi(t)\rangle \in \mathcal{H}$, where $\mathcal{H}$ denotes the Hilbert space,

such that $|\psi(\tau)\rangle = e^{i\phi}|\psi(0)\rangle$ for some real ϕ, defines a closed curve in the projective Hilbert space $\mathcal{P}$. Now if $\left|\tilde{\psi}(t)\right\rangle = e^{-if(t)}|\psi(t)\rangle$ such that $f(\tau) - f(0) = \phi$, then the geometric phase is given by

$$\beta = i \oint_\Gamma \left\langle \tilde{\psi} \middle| d\tilde{\psi} \right\rangle, \tag{24}$$

where Γ is the closed curve in the $\mathcal{P}$. Clearly, β is independent of the rate at which the system traverses Γ, hence the condition for adiabaticity is removed.

The kinematic approach of Mukunda-Simon [47] generalizes the definition of geometric phase to include non-cyclic evolutions of which Aharonov-Anandan phase (24) is a special case. If $\mathcal{C}$ is any one-parameter smooth curve of unit vectors $|\psi(s)\rangle \in \mathcal{H}$, where $s \in [s_1, s_2] \subset \mathbb{R}$, then the geometric phase associated with the corresponding curve $\mathscr{C} \subset \mathcal{P}$ is defined by the functional

$$\phi_g[\mathscr{C}] = \arg\langle\psi(s_1)|\psi(s_2)\rangle - \Im\int_{s_1}^{s_2} ds\,\langle\psi(s)|\dot{\psi}(s)\rangle\,, \tag{25}$$

where $\left|\dot{\psi}(s)\right\rangle$ denotes derivative with respect to s. The geometric phase $\phi_g[\mathscr{C}]$ can easily be shown to be gauge and reparametrization invariant. The two terms on the right hand side of (25) are respectively the total and dynamical phase associated with the curve $\mathcal{C}$, and the difference between the two gives geometric phase along $\mathscr{C}$.

We now use the definition (25) to calculate the geometric phases associated with the neutrino spin and spin-flavor evolution in a medium with uniformly twisting magnetic field and constant density as discussed in the previous Section. We will concern ourselves only with the two component formalism. If a neutrino is initially created in left-helicity state, i.e. $|\nu(0)\rangle = (1 \quad 0)^T$ then after traveling a distance z in the magnetic field the the neutrino eigenstate will be a mixture of left- and right-handed components and is given by $|\nu(z)\rangle = (\nu_L(z) \quad \nu_R(z))^T$. The geometric phase acquired by the state $|\nu(z)\rangle$, according to(25), is then given by

$$\phi_g^L(z) = arg\,\langle\nu(0)|\nu(z)\rangle - \Im\int_0^z \langle\nu(z')|\frac{d}{dz'}|\nu(z')\rangle\,dz'. \tag{26}$$

Using the expressions for $\nu_L(z)$ and $\nu_R(z)$, (10) and (11) respectively, we get the following expressions for the geometric phase

$$\begin{aligned}\phi_g^L(z) = &-\arctan\Big(\cos 2\theta_m \tan\frac{\delta E_m z}{2}\Big) + \frac{\delta E_m z}{2}\cos 2\theta_m \\ &+ \frac{\Delta\phi(z)}{2} - \frac{\dot{\phi}}{2}\Big(z\cos^2 2\theta_m + \sin^2 2\theta_m \frac{\sin\delta E_m z}{\delta E_m}\Big),\end{aligned} \tag{27}$$

where $\Delta\phi(z) = \phi(z) - \phi(0)$. Similarly if a neutrino is produced initially in the right-helicity state the geometric phase acquired is given by

$$\phi_g^R(z) = -\,\phi_g^L. \tag{28}$$

Hence the spin and spin-flavor evolution of neutrino helicity states involve non-zero geometric phases. Note that these expressions for geometric phases are valid regardless of whether the neutrino propagation is adiabatic or not, unlike the case of Berry phase which requires the propagation to be adiabatic.

A particular case is neutrino spin and spin-flavor evolution in a magnetic field along a fixed direction in the transverse plane. In that case, (27) and (28) reduce to

$$\phi_g^L(z)\big|_{\dot{\phi}=0} = -\arctan\Big(\cos 2\theta_m \tan\frac{\delta E_m z}{2}\Big) + \frac{\delta E_m z}{2}\cos 2\theta_m, \tag{29}$$

$$\phi_g^R(z)\big|_{\dot{\phi}=0} = \arctan\Big(\cos 2\theta_m \tan\frac{\delta E_m z}{2}\Big) - \frac{\delta E_m z}{2}\cos 2\theta_m. \tag{30}$$

Thus the variation of external parameters can have significant effect on the trajectory in the projective Hilbert space which manifests itself as geometric phases.

Let us now consider the geometric phase in the cyclic limit. Since according to (13), the oscillation has a length scale $L_{\rm osc} = 2\pi/\delta E_m$, neutrinos initially produced in a definite left- or right-handed state return to the original state after traveling distance a $L_{\rm osc}$, apart from a phase factor. For this cyclic process the geometric phases (27) and (28) become

$$\phi_{g,cyc}^L = -\,\pi(1-\cos 2\theta_m) + \frac{\Delta\phi}{2}(L_{osc}) - \frac{\dot{\phi}}{2}L_{osc}\cos 2\theta_m, \tag{31}$$

$$\phi_{g,cyc}^R = \pi(1-\cos 2\theta_m) - \frac{\Delta\phi}{2}(L_{osc}) + \frac{\dot{\phi}}{2}L_{osc}\cos 2\theta_m, \tag{32}$$

which are the cyclic Aharonov-Anandan phases as defined in (24). For the particular case of magnetic field in fixed direction the phases reduce to $\phi_g = \pm\pi(1-\cos 2\theta_m)$, which is the famous Aharonov-Anandan phase for spin-precession in constant magnetic field [43].

To analyze the behavior of geometric phases in neutrino spin and spin-flavor evolutions, we consider the particular case of solar neutrinos. The left-handed electron neutrinos produced in the inner regions of the Sun propagate outwards under the influence of matter and magnetic fields. As a first order calculation we assume a constant density and magnetic field profile for the Sun, and investigate the variation in geometric phase for different values of rotation frequency of the magnetic field, parametrized as $\dot{\phi} = \pi/fR$, where R is the radius of the Sun. We obtain the following plots for the two different cases of spin-precession $\nu_{eL} \to \nu_{eR}$ and spin-flavor precession $\nu_{eL} \to \nu_{\mu R}, \bar{\nu}_\mu$.

The following plots show that the geometric phase for the case of spin-precession $\nu_{eL} \to \nu_{eR}$ depends sensitively on the field rotation. For the case of $\dot{\phi} \neq 0$, ϕ_g^L shows rapid variation with distance while for the other case of magnetic field in a fixed direction field, ϕ_g^L remains constant over larger periods. For spin-flavor precession the

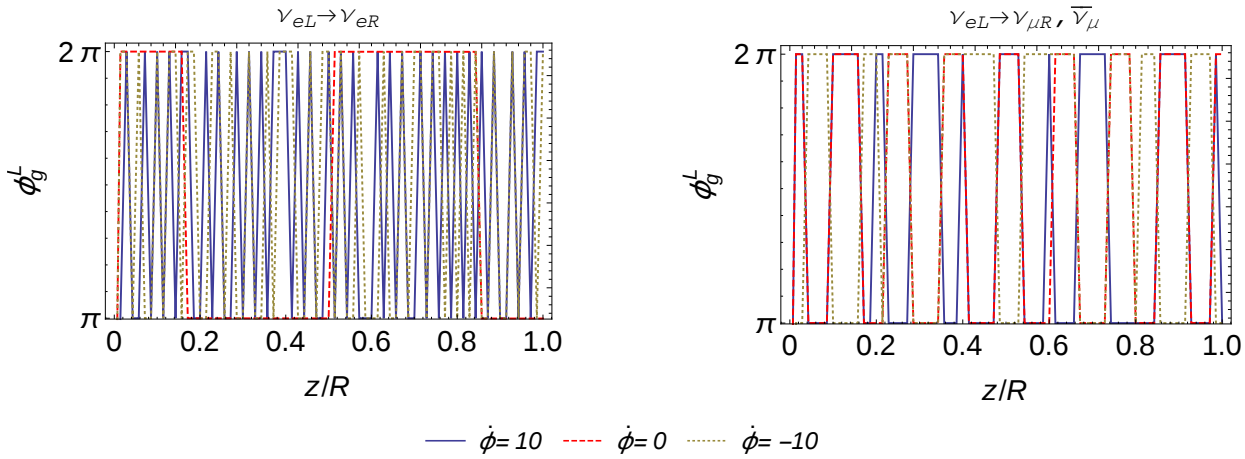

Figure 1: Geometric phases for neutrino propagation in Sun for different values of field rotation frequency for neutrino spin-precession $\nu_{eL} \to \nu_{eR}$ and spin-flavor precession $\nu_{eL} \to \nu_{\mu R}$. The rotation frequency is in units of π/R, and the positive and negative signs of $\dot{\phi}$ correspond to anticlockwise and clockwise rotation about the neutrino direction respectively. We used the following parameters $\Delta m^2 = 7.5 \times 10^{-5} eV^2$, $\theta = 33^\circ$, $E = 0.2 MeV$, $n_e \approx 10^{24} g/cm^3$, $B = 10^3 G$.

period of the phase is almost same for both rotating and fixed direction magnetic fields. Thus geometric phase shows quantitatively different behavior for neutrino spin and spin-flavor precession respectively.

Next we will study the neutrino spin and spin-flavor evolution in the case of a neutron star with realistic density and magnetic field profiles. We will examine various cases both inside and outside the neutron star and see the quantitative difference in geometric phases in different scenarios.

IV. Neutrino Propagation in Neutron Stars

When stars run out of nuclear fuel at the end of their lives, the core of the star collapses under its own gravity resulting in a supernova explosion. Neutron stars (NSs) are the compact objects which are formed as final remnants of the core collapse supernova of stars with mass of about 8-20 times the mass of the Sun. NSs contain some of the most extreme astrophysical environments where the interior densities can be $\sim 5 - 10$ times the nuclear saturation density ($\approx 2.8 \times 10^{14} g/cm^3$) and where magnetic fields from surface to the interiors can vary from $10^{15} - 10^{18} G$ [62, 63]. Although NS are primarily composed of neutrons, there are also small fraction of protons, electrons and other nuclei. In the interior where density exceeds nuclear saturation density exotic particles such as deconfined quarks, stable hyperon matter and superfluid pion condensate may appear [64, 65].

Neutrinos play an important role in the formation and subsequent cooling of NSs. During the first few seconds of the supernova collapse a large number of neutrinos diffuse through the resulting proto-NS which leads to a rapid drop in temperature by a factor of ~ 100. After about a minute, the NS becomes transparent to neutrinos resulting in further drop in temperatures. The main process by which the neutrinos are produced in the NS cores is so called direct Urca process $n \to p + e^- + \bar{\nu}_e$, $p + e^- \to n + \nu_e$[65, 66]. However the direct Urca process requires certain energy threshold below which the neutrino emission occurs via modified Urca process $n + (n,p) \to p + (n,p) + e^- + \bar{\nu}_e$, $p + (n,p) \to n + (n,p) + e^+ + \nu_e$ [67]. There are several other mechanisms by which neutrinos are produced in the NSs and help in the NS cooling (see [68] for a detailed review).

In the following we study the spin-flavor evolution of the neutrinos produced in the core region of the NS. For definiteness we consider only the left-handed electron neutrinos produced below the resonance region and calculate the geometric phases they acquire as they propagate in the interior regions of the NS and finally come out of it. We also study the effect of magnetic field rotation on the geometric phases and the probabilities of the spin and spin-flavor conversion. These calculations require the knowledge of the density and magnetic field profiles in the interior and outer regions of the NS. The knowledge of the exact density profile of NS depends strongly on the equation of state for which many models have been proposed (see [69] for a recent review). However without going into details of the models, we assume a simplistic density profile where the density decreases quadratically from the center

$$\rho Y_e^{\rm eff} = \begin{cases} \rho_0 + \rho_1 r^2, & \text{for } r \le R \\ 0 & \text{for } r > R \end{cases}, \qquad (33)$$

where R is the radius and ρ_0 is the central density of the NS. The values of radius and central density are taken as $R = 10\ km$ and $\rho_0 = 10^{15} g/cm^3$. The typical surface

density of the NS is $\sim 10^9 g/cm^3$ which determines the value of ρ_1.The magnetic field profile in the interior[70] and outer[20] regions of the NS are taken as

$$B(r) = \begin{cases} B_s + B_c\Big(1 - exp\Big(-\beta(\rho/\rho_s)^\gamma\Big)\Big) & \text{for } r \le R \\ B_s(R/r)^3 & \text{for } r > R \end{cases}, \tag{34}$$

where $\beta = 0.005$, $\gamma = 2$, $B_c = 10^{18}G$, $B_s = 10^{14}G$ and ρ_s is the nuclear saturation density.

A. Geometric phases

The neutrino spin-flavor evolution equation (4), excluding the effects of field rotation can be written as

$$i\frac{d}{dz}\begin{pmatrix}\nu_L \\ \nu_R\end{pmatrix} = \left(\frac{V(z)}{2}\sigma_3 + \mu B(z)\sigma_1\right)\begin{pmatrix}\nu_L \\ \nu_R\end{pmatrix}, \tag{35}$$

where

$$V = \frac{\sqrt{2}G_F\rho Y_e^{eff}}{m_N} - \frac{\Delta m^2}{2E}\cos 2\theta. \tag{36}$$

The formal solution of (35) is given by the evolution matrix

$$S(z, z_0) = \mathcal{P}\exp\left(-\frac{i}{2}\int_{z_0}^{z}(V(z')\sigma_3 + 2\mu B(z')\sigma_1)dz'\right), \tag{37}$$

where $\mathcal{P}$ is the path ordering operator. However as we will see, we can find the approximate solutions of (35) using the notion of adiabatic evolution. The Hamiltonian in (35) can be diagonalized by the transformation

$$|\nu\rangle = U_{in}\,|\psi\rangle\,, \tag{38}$$

where U_{in} is the rotation matrix

$$U_{in} = \begin{pmatrix}\cos\theta_{in} & -\sin\theta_{in} \\ \sin\theta_{in} & \cos\theta_{in}\end{pmatrix}. \tag{39}$$

The evolution equation (35) now becomes

$$i\frac{d}{dz}\begin{pmatrix}\psi_1 \\ \psi_2\end{pmatrix} = \begin{pmatrix}\sqrt{\left(\frac{V}{2}\right)^2 + (\mu B)^2} & -id\theta_{in}/dz \\ id\theta_{in}/dz & -\sqrt{\left(\frac{V}{2}\right)^2 + (\mu B)^2}\end{pmatrix}\begin{pmatrix}\psi_1 \\ \psi_2\end{pmatrix}. \tag{40}$$

The diagonalization condition gives the mixing angle

$$\tan 2\theta_{in} = -\frac{2\mu B}{V}. \tag{41}$$

For the given density and magnetic field profiles inside the NS, value of the mixing angle $\theta_{in}(z) \ll 1$, which shows the dominance of the matter term compared to the magnetic field term. Now we calculate the parameter

$$\gamma = \frac{\sqrt{(V/2)^2 + (\mu B)^2}}{|d\theta_{in}/dz|} \tag{42}$$

for the given density (33) and magnetic field profiles (34) and find that $\gamma \gg 1$ for the region inside the NS, so the adiabaticity condition holds and we can write the solutions of (40) as

$$\psi_1(z) \approx \exp\left(-i\int_{z_0}^{z}dz'\sqrt{\left(\frac{V}{2}\right)^2 + (\mu B)^2}\right)\psi_1(z_0), \tag{43}$$

$$\psi_2(z) \approx \exp\left(i\int_{z_0}^{z}dz'\sqrt{\left(\frac{V}{2}\right)^2 + (\mu B)^2}\right)\psi_2(z_0). \tag{44}$$

Thus under adiabatic conditions $\psi_1(z)$ and $\psi_2(z)$ are the instantaneous eigenstates of the Hamiltonian and are related to $\nu_L(z)$, $\nu_R(z)$ as

$$\nu_L(z) = \cos\theta_{in}\psi_1(z) - \sin\theta_{in}\psi_2(z), \tag{45}$$

$$\nu_R(z) = \sin\theta_{in}\psi_1(z) + \cos\theta_{in}\psi_2(z). \tag{46}$$

Considering the case of left-handed electron neutrinos produced near the center of the NS, we have the initial conditions

$$\begin{pmatrix}\nu_L \\ \nu_R\end{pmatrix} = \begin{pmatrix}1 \\ 0\end{pmatrix} = \begin{pmatrix}\cos\theta_{in}(z_0) & -\sin\theta_{in}(z_0) \\ \sin\theta_{in}(z_0) & \cos\theta_{in}(z_0)\end{pmatrix}\begin{pmatrix}\psi_1(z_0) \\ \psi_2(z_0)\end{pmatrix}, \tag{47}$$

which give

$$\psi_1(z_0) = \cos\theta_{in}(z_0), \qquad \psi_2(z_0) = -\sin\theta_{in}(z_0). \tag{48}$$

The geometric phase associated with state a $|\nu(z)\rangle = (\nu_L(z) \quad \nu_R(z))^T$ is then given by (25) as

$$\phi_g(z) = \arg\langle\nu(z_0)|\nu(z)\rangle - \Im\int_{z_0}^{z}dz'\,\langle\nu(z')|\frac{d}{dz'}\nu(z')\rangle\,. \tag{49}$$

Using (45) and (48) we get the expression for ϕ_g as

$$\begin{aligned}\phi_g(z) = &-\arctan\left[\tan\zeta(z)\left(\frac{\cos(\theta_{in}(z) - \cos\theta_{in}(z_0))}{\cos(\theta_{in}(z) + \cos\theta_{in}(z_0))}\right)\right] \\ &+ \cos 2\theta_{in}(z_0)\int_{z_0}^{z}\zeta'(z')dz' \\ &- \sin 2\theta(z_0)\int_{z_0}^{z}\sin 2\zeta(z)\frac{d\theta_{in}(z')}{dz'},\end{aligned} \tag{50}$$

where

$$\zeta(z) = \int_{z_0}^{z}dz'\sqrt{\left(\frac{V(z')}{2}\right)^2 + (\mu B(z'))^2}, \tag{51}$$

and $\zeta'(z)$ is the derivative with respect to z. The dominant term in expression (50) is the second term $\zeta(z) - \zeta(z_0)$ and in comparison the third term can be neglected. So we can write (50) as

$$\begin{aligned}\phi_g(z) = &-\arctan\left[\tan\zeta(z)\left(\frac{\cos(\theta_{in}(z) - \cos\theta_{in}(z_0))}{\cos(\theta_{in}(z) + \cos\theta_{in}(z_0))}\right)\right] \\ &+ \cos 2\theta_{in}(z_0)(\zeta(z) - \zeta(z_0)), \quad z \le R.\end{aligned} \tag{52}$$

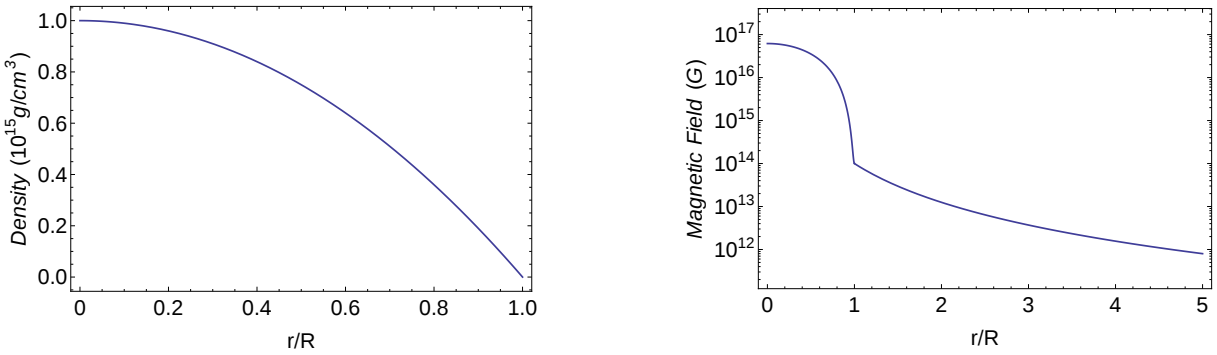

Figure 2: Density and magnetic field profiles of the neutron star. Magnetic field is plotted in log scale

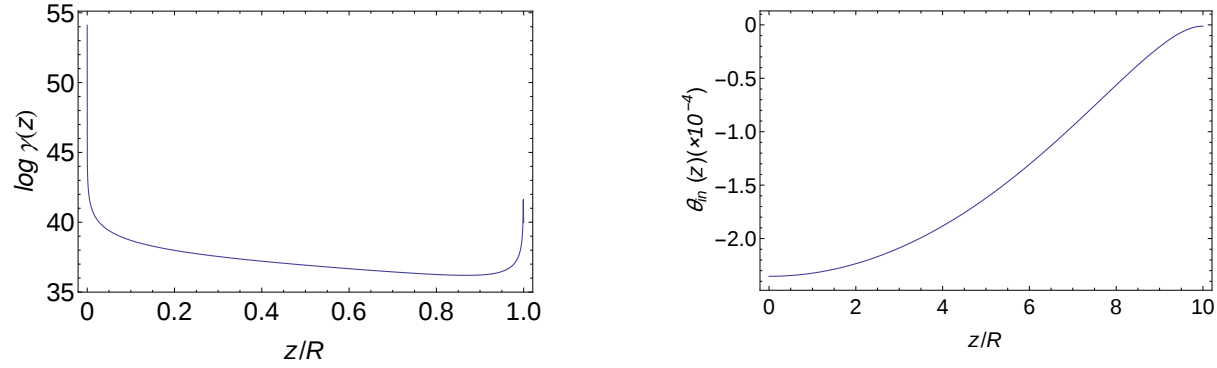

Figure 3: $\log\gamma(z)$ and $\theta_{in}(z)$ as a function of distance inside the NS. As we can see $\gamma \gg 1$ for the region inside the NS, so adiabatic approximation holds well. Also θ_{in} is sufficiently small so we can take $\sin\theta_{in} \approx \theta_{in}$ and $\cos\theta_{in} \approx 1$.

As the neutrinos come out of the NS, the matter effects vanish so the potential term (36) $V \to -\Delta m^2 \cos 2\theta/2E$. First we consider the case of spin-flavor precession for which we calculate the adiabaticity parameter γ defined in (42) and find that $\gamma \gg 1$ for all the points along the neutrino trajectory outside the NS. So adiabatic approximation holds and we can write the solutions of the spin-flavor evolution equation (35) in the region $z > R$ as

$$\nu_L(z) = \cos\theta_{out}\psi_1(z) - \sin\theta_{out}\psi_2(z), \tag{53}$$

$$\nu_R(z) = \sin\theta_{out}\psi_1(z) + \cos\theta_{out}\psi_2(z), \tag{54}$$

where now

$$\psi_1(z) \approx \exp\left(-i\int_R^z dz' \sqrt{\left(\frac{\Delta m^2}{4E}\right)^2 + (\mu B(z'))^2}\right)\psi_1(R), \tag{55}$$

$$\psi_2(z) \approx \exp\left(i\int_R^z dz' \sqrt{\left(\frac{\Delta m^2}{4E}\right)^2 + (\mu B(z'))^2}\right)\psi_2(R), \tag{56}$$

$$\theta_{out} = \frac{1}{2}\arctan\left(\frac{4E\mu B}{\Delta m^2}\right). \tag{57}$$

As we will see later the transition probability $\nu_L \to \nu_R$ inside the NS is negligible so the neutrinos produced initially in left-handed state will remain in the same state as they reach the surface of the NS, so we have the conditions

$$\begin{pmatrix}\nu_L\\ \nu_R\end{pmatrix} = \begin{pmatrix}1\\ 0\end{pmatrix} = \begin{pmatrix}\cos\theta_{out} & -\sin\theta_{out}\\ \sin\theta_{out} & \cos\theta_{out}\end{pmatrix}\begin{pmatrix}\psi_1(R)\\ \psi_2(R)\end{pmatrix}, \tag{58}$$

which give

$$\psi_1(R) = \cos\theta(R) = \pi/4, \quad \psi_2(R) = -\sin\theta(R) = -\pi/4. \tag{59}$$

The geometric phase associated with state $|\nu(z)\rangle$ is given by

$$\phi_g^{sf}(z) = \arctan\left(\frac{\sin\theta_{out}(z) - \cos\theta_{out}(z)}{\sin\theta_{out}(z) + \cos\theta_{out}(z)}\tan\chi(z)\right) - \frac{\pi^2}{8}\int_R^z dz' \sin 2\chi(z')\frac{d\theta_{out}(z')}{dz'}, \quad z > R \tag{60}$$

where

$$\chi(z) = \int_R^z dz' \sqrt{\left(\frac{\Delta m^2}{4E}\right)^2 + (\mu B(z'))^2}. \tag{61}$$

For distances $z > 100R$, θ_{out} is sufficiently small, so we can approximate $\sin\theta_{out} \approx \theta_{out}$ and $\cos\theta_{out} \approx 1$. So according to (60), we can write the geometric phase for

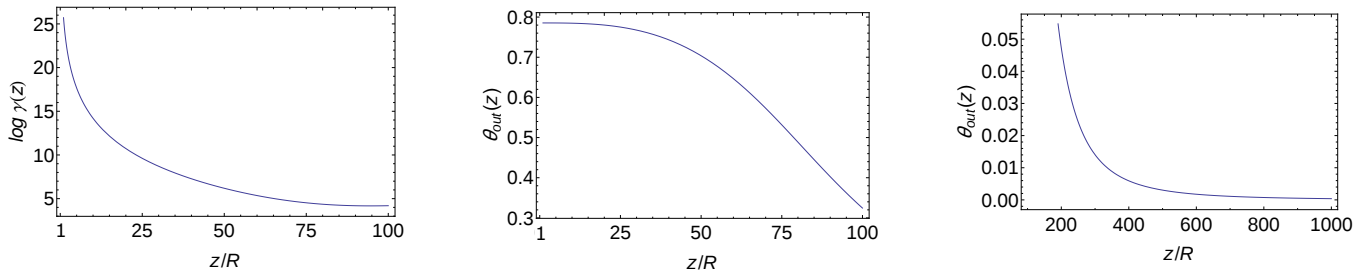

Figure 4: Adiabaticity parameter $\log\gamma(z)$ and $\theta_{out}(z)$ as a function of distance outside the NS. The adiabaticity parameter is sufficiently large, so the adiabatic approximation holds. For large distances $z \gg R$, θ_{out} is very small so we can take $\sin\theta_{out} \approx \theta_{out}$ and $\cos\theta_{out} \approx 1$.

distances $z \gg R$ as

$$\phi_g^{sf}(z) = \arctan\left\{\left(\frac{\theta_{out}-1}{\theta_{out}+1}\right)\tan\chi(z)\right\} - \frac{\pi^2}{8}\int_{z>100R}^{z} dz'\ \sin 2\chi(z')\frac{d\theta_{out}(z')}{dz'}. \quad (62)$$

We now consider the case of spin-precession $\nu_{eL} \to \nu_{eR}$ as neutrinos emerge from the NS. Since, for pure spin-precession in vacuum $V = 0$, the adiabaticity parameter (42) is now $\gamma = \mu B/|d\theta_{out}/dz|$. According to (57) as $V \to 0$, $\theta_{out} \to \pi/2$ thus $\gamma \to \infty$, i.e. we have the extreme adiabatic limit. In this case the second term in (60) vanishes and we get a simple result

$$\phi_g^{spin}(z) = \frac{\mu B_s R}{2}\Big(1 - \frac{R^2}{z^2}\Big), \quad z > R. \quad (63)$$

For large distances $z \gg R$, the second term in bracket becomes vanishingly small, entailing the asymptotic limit:

$$\phi_g^{spin} = \frac{\mu B_s R}{2}, \quad z \to \infty. \quad (64)$$

Even at large distances a neutrino eigenstate carries a geometric phase acquired during the spin-precession in the magnetic field of the NS, which in principle, is a detectable quantity. The above simple result connects the three basic parameters μ, B_s and R. For the parameter we have considered, the value of the phase comes out a large value $\sim 10^5$ and may average out to zero for large distances. However, since the parameters B_s and R depend on the particular NS, there can be cases where the surface magnetic field $B_s \sim 10^9 - 10^{10}G$. For such cases the variation in the geometric phase will be sufficiently small enough to be a measurable quantity. Also according to (64), even magnetic moment as small as $10^{-16}\mu_B$ can give rise to significant geometric phase for $B_s \sim 10^{14}G$ in the NS environments.

B. Effects of field rotation

If the magnetic field is rotating in the transverse plane with angular velocity $\dot\phi$ about the neutrino direction then the geometric phase (52) modifies to

$$\phi_g^{rot}(z) = \phi_g(z)\big|_{V\to V+\dot\phi} + \frac{\Delta\phi}{2} - \frac{\dot\phi}{2}\Big(\cos 2\theta_{in}(z_0)\int_{z_0}^{z} dz'\cos 2\theta_{in}(z) + \sin 2\theta_{in}(z_0)\int_{z_0}^{z} dz'\sin 2\theta_{in}(z')\cos 2\zeta(z')\Big), \quad z \le R \quad (65)$$

where the first term refers to the geometric phase in the non-rotating case obtained with replacement $V \to V + \dot\phi$ and $\Delta\phi = \phi(z) - \phi(z_0)$. The potential term inside the NS can be written as

$$V(z) = \Big(-\frac{\Delta m^2}{2E}\cos 2\theta + \frac{\sqrt{2}G_F\rho_0}{m_N} + \dot\phi\Big) + \frac{\sqrt{2}G_F\rho_1}{m_N}z^2. \quad (66)$$

Now, if the magnetic field undergoes n half rotations at a fraction f of the radius R of the neutron star, then

$$\dot\phi = 2\times 10^{-17}\Big(\frac{n\pi}{f}\Big)\text{MeV}. \quad (67)$$

For the given density profile the second term in the bracket in (66) is

$$\sqrt{2}G_F\rho_0/m_N = 7.54\times 10^{-5}\text{MeV}. \quad (68)$$

Clearly, for (67) to be comparable to (68), n/f must be $\sim 10^{10}$, i.e., the field must rotate by π every 10 nm or so. We assume that such high frequencies are not encountered and the $\dot\phi$ term can be neglected in (66). So the first term in (65) is the same as (52). In the limit of small $\theta_{in}(z_0)$, (65) reduces to

$$\phi_g^{rot}(z) = \phi_g(z) + \frac{\Delta\phi}{2} - \frac{\dot\phi}{2}\int_{z_0}^{z} dz'\cos\theta(z'), \quad z \le R. \quad (69)$$

For the case of spin-flavor precession outside the NS the potential is given by

$$V(z) = -\Delta m^2\cos 2\theta/2E + \dot\phi. \quad (70)$$

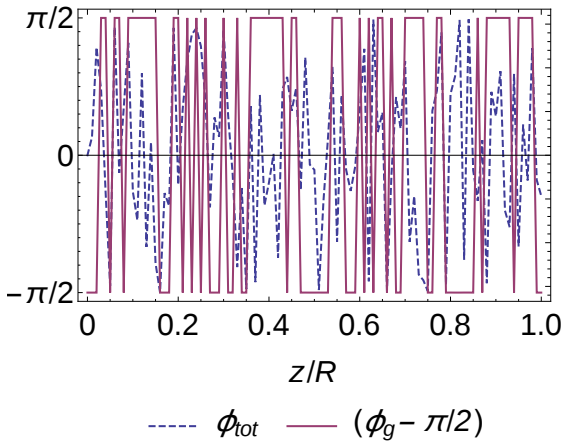

(a) Inside, $\nu_{eL} \to \nu_{eR}, \nu_{\mu R}, \bar{\nu}_{\mu}$

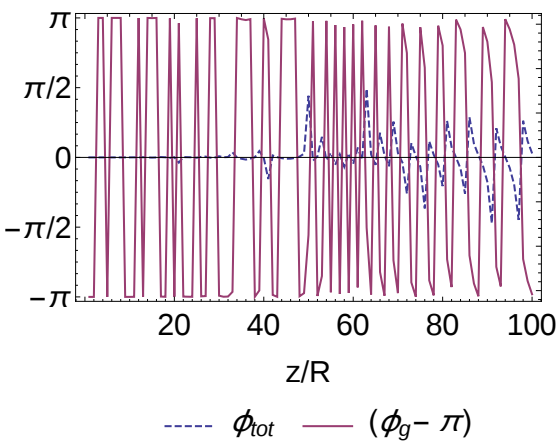

(b) Outside, $\nu_{eL} \to \nu_{\mu R}, \bar{\nu}_{\mu}$

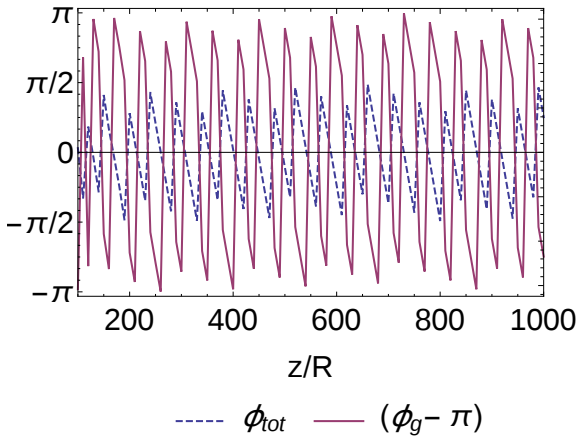

(c) Outside, $z >> R$, $\nu_{eL} \to \nu_{\mu R}, \bar{\nu}_{\mu}$,

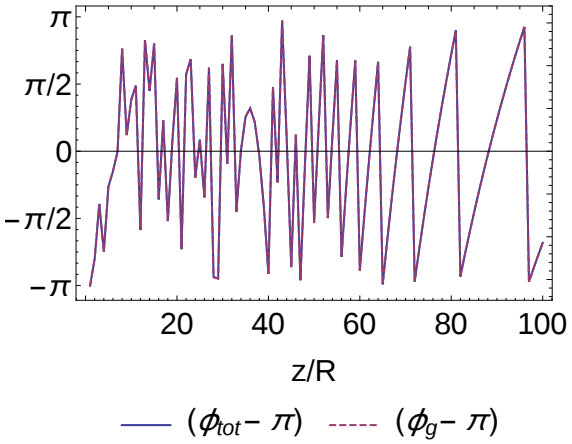

(d) Outside, $\nu_{eL} \to \nu_{eR}$

Figure 5: Variation of Geometric and total phases with distance for different cases inside and outside the NS. The geometric phases show quantitative different behavior for the above cases. Inside the NS, the variation of ϕ_g is limited to range $(0, \pi)$ while in the outside region it show variation in the full $(0, 2\pi)$ range. With regards to the type of precession, it can be seen that in the case of simple spin-precession $\nu_L \to \nu_R$, the entire phase is in geometric form, while for the case of spin-flavor precession ϕ_{tot} has a non-zero component in addition to ϕ_g.

The expression for the geometric phase becomes

$$\begin{aligned}\phi_g^{sf,rot}(z) = &\arctan\left(\frac{\sin\theta_{out}(z) - \cos\theta_{out}(z)}{\sin\theta_{out}(z) + \cos\theta_{out}(z)}\tan\chi(z)\right) \\ &+ \frac{\Delta\phi}{2} - \left(\frac{\pi}{4}\right)^2 \int_R^z dz' \big(2\sin 2\chi(z')\frac{d\theta_{out}}{dz'} \\ &+ \sin 2\theta_{out}(z')\cos 2\chi(z')\big), \quad z > R\end{aligned} \tag{71}$$

where now

$$\theta_{out}(z) = -\frac{1}{2}\arctan\left(\frac{2\mu B}{-\Delta m^2/2E + \dot{\phi}}\right), \quad \text{and} \tag{72}$$

$$\chi(z) = \int_R^z dz' \sqrt{\Big(-\frac{\Delta m^2}{4E} + \frac{\dot{\phi}}{2}\Big)^2 + (\mu B(z'))^2}. \tag{73}$$

The above expression also give the geometric phase for the case of spin-precession in the limit of vanishing Δm^2. The following plots show the effects of the magnetic field rotation on the geometric phases for different values of rotation frequency.

C. Transition probabilities and cross boundary effect

Under adiabatic approximation the survival probability of the right and left handed neutrino states inside the

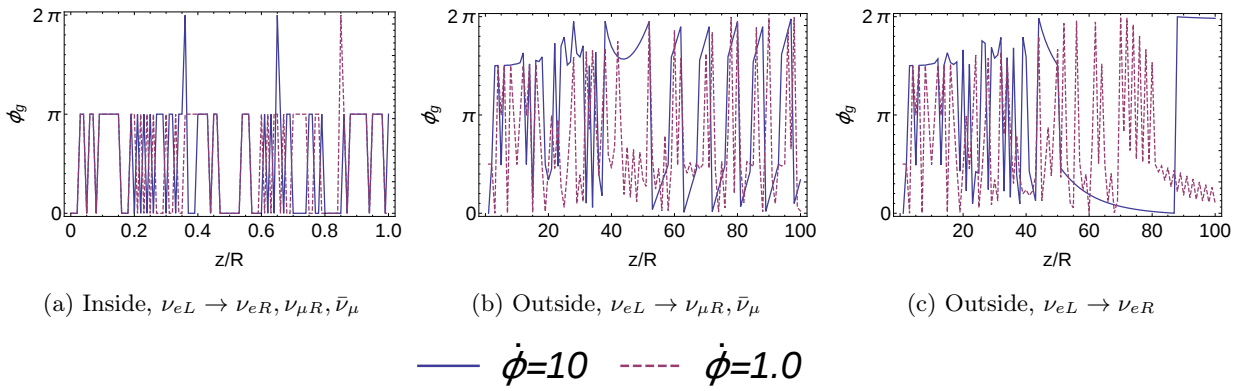

(a) Inside, $\nu_{eL} \to \nu_{eR}, \nu_{\mu R}, \bar{\nu}_\mu$ (b) Outside, $\nu_{eL} \to \nu_{\mu R}, \bar{\nu}_\mu$ (c) Outside, $\nu_{eL} \to \nu_{eR}$

Figure 6: Effects of rotation on geometric phases for different values of field rotation frequency. For the inside regions ϕ_g shows almost same behavior for different rotation frequency, while for the outside case the variation of ϕ_g is markedly different for different values of rotation frequency.

neutron star to order θ are given by

$$P_{in}(\nu_L \to \nu_L)(z) = |\nu_L(z)|^2 = 1 + 2\theta_{in}(z_0)\theta_{in}(z)\cos 2\zeta(z), \quad \text{z} \leq \text{R}. \tag{74}$$

For given values of $\theta(z)$, $V(z)$ and $B(z)$, the probability $P(\nu_L \to \nu_L)(z) \approx 1$ and $P(\nu_L \to \nu_R)(z) \approx 0$, so there are almost no transitions inside the NS. For the outside case the situation is more interesting

$$P_{out}(\nu_L \to \nu_L)(z) = \frac{1}{2}\big(1 + \cos 2\theta_{out}(z)\cos 2\theta_{out}(R) + \sin 2\theta_{out}(z)\sin 2\theta_{out}(R)\cos 2\chi(z)\big), \quad \text{z} > \text{R}. \tag{75}$$

The oscillations in probability arise due to the last term in the bracket. As can be seen in Figure 7, the effective oscillation length outside the NS $\sim 10cm$. After a distance of about $250R$ the survival probability converges to one-half. Thus after traveling a distance of $\sim 250R$, half of the left-handed neutrinos produced inside the NS are converted to the right-handed neutrinos.

For the case of neutrino propagation in a medium of constant density and uniformly twisting magnetic fields, one can define a critical magnetic field, which is the magnetic field required for the oscillation amplitudes $\nu_L \to \nu_R$ to be close to unity and is given by [20]

$$B_{cr}[G] = 43\left(\frac{\mu_B}{\mu}\right)\left|\left(\frac{\Delta m^2}{1eV^2}\right)\left(\frac{MeV}{E}\right)\cos 2\theta - 2.5\times 10^{-31}\left(\frac{n_{eff}}{cm^{-3}}\right) + 0.4\left(\frac{\dot{\phi}}{m}\right)\right|, \tag{76}$$

In the interior regions of the neutron star, $\rho \approx 10^{15} g/cm^3$ gives $n_{eff} \approx 6\times 10^{38} cm^{-3}$, hence for neutrinos with energy $E = 1MeV$, (76) gives $B_{cr} \approx 6\times 10^{20} G$. Since $B_{cr} \gg B$ in the interior of the neutron star, so the transitions are negligible. Even in the outermost crust of the star, $n_{\text{eff}} \approx 10^{33} cm^{-3}$, and $B_{cr} \approx 10^{15} G$, which is greater than the magnetic fields prevailing in those regions. So we expect very weak neutrino transitions inside the neutron stars in the case of neutrinos produced below the resonance regions. For the regions just outside the neutron star density suddenly drops to zero, so there is sharp decrease in the critical magnetic field required for the helicity transitions. For 1 MeV neutrinos, (76) gives $B_{cr} = 10^8 G$. Since the magnetic field just outside the neutron star is $\sim 10^{14} G (>> B_{cr})$, as the neutrinos cross the surface of the NS, there are rapid helicity transitions which is termed as cross boundary effect[20].

Since the magnetic field outside the NS falls off as $1/r^3$, the range over which the magnetic field exceeds critical magnetic field is given by $r_{cr} = R(B/B_{cr})^{1/3} \approx 100R$. As can be seen in Figure 7, the oscillation amplitude reduces as we go away from the NS and almost vanishes for $r > 250R$ in case for non-rotating fields. If we consider the effect of field rotation then according to (76) the critical magnetic field required to sustain oscillations increases. For $\dot{\phi} = 10$, the $B_{cr} \approx 6\times 10^8 G$. Thus the range over which oscillation amplitudes are finite decreases to $\approx 50R$.

V. Conclusions

We have studied the non-cyclic geometric phases associated with neutrino spin and spin-flavor transitions. First, we derived analytical expressions of non-cyclic geometric phases for the case of neutrino oscillations in a medium with constant density and uniformly rotating magnetic field. It was shown that in the limiting case of non-rotating magnetic fields, the expressions reduce to the usual Aharonov-Anandan phases. As a particular case, we analyzed the geometric phases acquired by the solar neutrinos as they propagate outwards under the effect of matter and magnetic fields. We showed that for spin precession $\nu_{eL} \to \nu_{eR}$, the geometric phases depends strongly on the rotation frequency of the magnetic field,

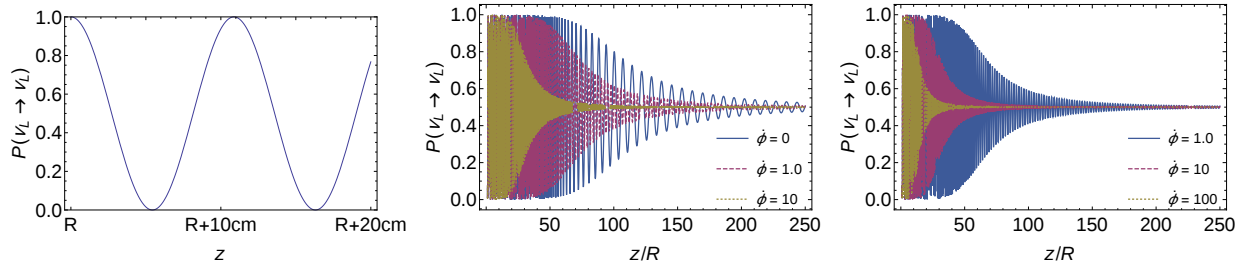

(a) Oscillation length scale outside the NS

(b) Spin-flavor transition probability, $\nu_{eL} \to \nu_{\mu R}, \bar{\nu}_{\mu}$

(c) Spin transition probability, $\nu_{eL} \to \nu_{eR}$

Figure 7: The survival probability of spin and spin-flavor precession for various values of the rotation frequency. Larger values of field rotation leads to more rapid transitions and the probability converge at a faster rate to the value 0.5 for both spin and spin-flavor conversions.

while for spin-flavor precession $\nu_{eL} \to \nu_{\mu R}, \bar{\nu}_{\mu}$ the magnitude of the rotation does not have much significant effect on the geometric phases.

Further, we analyzed the particular situation of neutrinos produced in the NS, propagating outwards under the effect of matter and magnetic fields. We derived analytical expressions of the non-cyclic geometric phases and studied their behavior both inside and outside the NS for various cases. In particular we showed that for neutrinos produced inside the NS, the neutrino eigenstates carry non-vanishing geometric phases even at large(infinite) distances from their point of production which it turn depends on the strength of the magnetic fields prevailing in those environments. We also studied the transition probability and the cross boundary effects and showed that at a distance of about 250 times the radius of the NS, the initial flux of left handed neutrinos produced inside the NS is reduced by a factor of one-half. We would like to point out that we considered only the case of neutrinos produced below resonance regions. However, in more realistic situations there can be significant resonant effects due to both matter and magnetic fields and it would be interesting to explore these effects in the context of geometric phases.

The emergence of geometric phases in neutrino spin and spin-flavor evolution highlights an important geometric aspect of this phenomena. Even though at present there seems to be no method to detect such phases in the current experiments, the present calculations suggest that the neutrino eigenstates carry significant information about geometric phases, which is well worth exploring.

[1] Y. Fukuda *et al.* (Super-Kamiokande), Phys. Rev. Lett. **81**, 1562 (1998), arXiv:hep-ex/9807003 [hep-ex]; Q. R. Ahmad *et al.* (SNO), Phys. Rev. Lett. **87**, 071301 (2001), arXiv:nucl-ex/0106015 [nucl-ex]; Phys. Rev. Lett. **89**, 011301 (2002), arXiv:nucl-ex/0204008 [nucl-ex].

[2] W. J. Marciano and A. I. Sanda, Phys. Lett. **B67**, 303 (1977).

[3] B. W. Lee and R. E. Shrock, Phys. Rev. **D16**, 1444 (1977).

[4] B. Kayser, Phys. Rev. **D26**, 1662 (1982).

[5] K. Fujikawa and R. Shrock, Phys. Rev. Lett. **45**, 963 (1980).

[6] J. Schechter and J. W. F. Valle, Phys. Rev. **D24**, 1883 (1981), [Erratum: Phys. Rev.D25,283(1982)].

[7] S. P. Mikheev and A. Yu. Smirnov, Sov. Phys. JETP **64**, 4 (1986), [Zh. Eksp. Teor. Fiz.91,7(1986)], arXiv:0706.0454 [hep-ph].

[8] C.-S. Lim and W. J. Marciano, Phys. Rev. **D37**, 1368 (1988).

[9] E. K. Akhmedov, Phys. Lett. **B213**, 64 (1988).

[10] E. K. Akhmedov and M. Yu. Khlopov, Mod. Phys. Lett. **A3**, 451 (1988).

[11] J. Pulido, Phys. Rev. **D41**, 2956 (1990).

[12] A. B. Balantekin, P. J. Hatchell, and F. Loreti, Phys. Rev. **D41**, 3583 (1990).

[13] E. K. Akhmedov, A. Yu. Smirnov, and P. I. Krastev, Z. Phys. **C52**, 701 (1991).

[14] P. B. Pal, Int. J. Mod. Phys. **A7**, 5387 (1992).

[15] E. K. Akhmedov, S. T. Petcov, and A. Yu. Smirnov, Phys. Rev. **D48**, 2167 (1993), arXiv:hep-ph/9301211 [hep-ph].

[16] M. M. Guzzo and J. Pulido, Phys. Lett. **B317**, 125 (1993).

[17] O. G. Miranda, C. Pena-Garay, T. I. Rashba, V. B. Semikoz, and J. W. F. Valle, Nucl. Phys. **B595**, 360 (2001), arXiv:hep-ph/0005259 [hep-ph].

[18] J. Barranco, O. G. Miranda, T. I. Rashba, V. B. Semikoz, and J. W. F. Valle, Phys. Rev. **D66**, 093009 (2002), arXiv:hep-ph/0207326 [hep-ph].

[19] M. B. Voloshin, Phys. Lett. **B209**, 360 (1988).

[20] G. G. Likhachev and A. I. Studenikin, J. Exp. Theor. Phys. **81**, 419 (1995), [Zh. Eksp. Teor. Fiz.108,769(1995)].

[21] E. K. Akhmedov, A. Lanza, S. T. Petcov, and D. W. Sciama, Phys. Rev. **D55**, 515 (1997), arXiv:hep-ph/9603443 [hep-ph].

[22] S. Ando and K. Sato, JCAP **0310**, 001 (2003), arXiv:hep-ph/0309060 [hep-ph].
[23] A. Ahriche and J. Mimouni, JCAP **0311**, 004 (2003), arXiv:astro-ph/0306433 [astro-ph].
[24] E. K. Akhmedov and T. Fukuyama, JCAP **0312**, 007 (2003), arXiv:hep-ph/0310119 [hep-ph].
[25] C. Giunti and A. Studenikin, Rev. Mod. Phys. **87**, 531 (2015), arXiv:1403.6344 [hep-ph].
[26] N. Nakagawa, Annals Phys. **179**, 145 (1987).
[27] J. Vidal and J. Wudka, Phys. Lett. **B249**, 473 (1990).
[28] C. Aneziris and J. Schechter, Int. J. Mod. Phys. **A6**, 2375 (1991).
[29] A. Yu. Smirnov, Phys. Lett. **B260**, 161 (1991).
[30] V. A. Naumov, Int. J. Mod. Phys. **D1**, 379 (1992).
[31] M. M. Guzzo and J. Bellandi, Phys. Lett. **B294**, 243 (1992).
[32] V. A. Naumov, Phys. Lett. **B323**, 351 (1994).
[33] M. Blasone, P. A. Henning, and G. Vitiello, Phys. Lett. **B466**, 262 (1999), arXiv:hep-th/9902124 [hep-th].
[34] X.-B. Wang, L. C. Kwek, Y. Liu, and C. H. Oh, Phys. Rev. **D63**, 053003 (2001), arXiv:hep-ph/0006204 [hep-ph].
[35] X.-G. He, X.-Q. Li, B. H. J. McKellar, and Y. Zhang, Phys. Rev. **D72**, 053012 (2005), arXiv:hep-ph/0412374 [hep-ph].
[36] Z. Y. Law, A. H. Chan, and C. H. Oh, Phys. Lett. **B648**, 289 (2007).
[37] P. Mehta, Phys. Rev. **D79**, 096013 (2009), arXiv:0901.0790 [hep-ph].
[38] J. Dajka, J. Syska, and J. Luczka, Phys. Rev. **D83**, 097302 (2011), arXiv:1309.7628 [hep-ph].
[39] S. Joshi and S. R. Jain, Phys. Lett. **B754**, 135 (2016), arXiv:1601.05255 [hep-ph].
[40] A. Capolupo, S. M. Giampaolo, B. C. Hiesmayr, and G. Vitiello, (2016), arXiv:1610.08679 [hep-ph].
[41] L. Johns and G. M. Fuller, Phys. Rev. **D95**, 043003 (2017), arXiv:1612.06940 [hep-ph].
[42] M. V. Berry, Proc. Roy. Soc. Lond. **A392**, 45 (1984).
[43] Y. Aharonov and J. Anandan, Phys. Rev. Lett. **58**, 1593 (1987).
[44] J. Samuel and R. Bhandari, Phys. Rev. Lett. **60**, 2339 (1988).
[45] I. J. R. Aitchison and K. Wanelik, Proc. Roy. Soc. Lond. **A439**, 25 (1992).
[46] A. K. Pati, Phys. Lett. **A202**, 40 (1995).
[47] N. Mukunda and R. Simon, Annals Phys. **228**, 205 (1993).
[48] S. Pancharatnam, in *Proceedings of the Indian Academy of Sciences-Section A*, Vol. 44 (Springer, 1956) pp. 398–417.
[49] C. A. Mead, Rev. Mod. Phys. **64**, 51 (1992).
[50] T. Bitter and D. Dubbers, Phys. Rev. Lett. **59**, 251 (1987).
[51] A. Tomita and R. Y. Chiao, Phys. Rev. Lett. **57**, 937 (1986).
[52] C. Pedder, J. Sonner, and D. Tong, Phys. Rev. **D77**, 025009 (2008), arXiv:0709.0731 [hep-th].
[53] A. Capolupo, Phys. Rev. **D84**, 116002 (2011), arXiv:1112.1337 [hep-ph].
[54] A. Capolupo, G. Lambiaseand, and G. Vitiello, Adv. High Energy Phys. **2015**, 826051 (2015), arXiv:1510.07288 [hep-ph].
[55] A. G. Beda, V. B. Brudanin, V. G. Egorov, D. V. Medvedev, V. S. Pogosov, M. V. Shirchenko, and A. S. Starostin, Adv. High Energy Phys. **2012**, 350150 (2012); A. G. Beda, V. B. Brudanin, V. G. Egorov, D. V. Medvedev, V. S. Pogosov, E. A. Shevchik, M. V. Shirchenko, A. S. Starostin, and I. V. Zhitnikov, Phys. Part. Nucl. Lett. **10**, 139 (2013).
[56] B. C. Canas, O. G. Miranda, A. Parada, M. Tortola, and J. W. F. Valle, Phys. Lett. **B753**, 191 (2016), [Addendum: Phys. Lett.B757,568(2016)], arXiv:1510.01684 [hep-ph].
[57] C. Giunti, K. A. Kouzakov, Y.-F. Li, A. V. Lokhov, A. I. Studenikin, and S. Zhou, Annalen Phys. **528**, 198 (2016), arXiv:1506.05387 [hep-ph].
[58] V. Bargmann, L. Michel, and V. L. Telegdi, Phys. Rev. Lett. **2**, 435 (1959).
[59] A. M. Egorov, A. E. Lobanov, and A. I. Studenikin, Phys. Lett. **B491**, 137 (2000), arXiv:hep-ph/9910476 [hep-ph].
[60] L. Wolfenstein, Phys. Rev. **D17**, 2369 (1978).
[61] L. B. Okun, M. B. Voloshin, and M. I. Vysotsky, *In *Bahcall, J. (ed.) et al.: Solar neutrinos* 344-350*, Sov. Phys. JETP **64**, 446 (1986), [Zh. Eksp. Teor. Fiz.91,754(1986)].
[62] V. V. Usov, Nature **357**, 472 (1992).
[63] D. Lai and S. L. Shapiro, Astrophys. J. **383**, 745 (1991).
[64] G. Baym and C. Pethick, Ann. Rev. Nucl. Part. Sci. **25**, 27 (1975).
[65] J. M. Lattimer and M. Prakash, Science **304**, 536 (2004), arXiv:astro-ph/0405262 [astro-ph].
[66] S. L. Shapiro and S. A. Teukolsky, *Black holes, white dwarfs, and neutron stars: The physics of compact objects* (Wiley (1983)).
[67] H.-Y. Chiu and E. E. Salpeter, Phys. Rev. Lett. **12**, 413 (1964).
[68] D. G. Yakovlev, A. D. Kaminker, O. Y. Gnedin, and P. Haensel, Phys. Rept. **354**, 1 (2001), arXiv:astro-ph/0012122 [astro-ph].
[69] J. M. Lattimer and M. Prakash, Phys. Rept. **621**, 127 (2016), arXiv:1512.07820 [astro-ph.SR].
[70] D. Bandyopadhyay, S. Chakrabarty, and S. Pal, Phys. Rev. Lett. **79**, 2176 (1997), arXiv:astro-ph/9703066 [astro-ph].